Journal of Molecular and Cellular Cardiology 46 (2009) 385–394

Contents lists available at ScienceDirect

Journal of Molecular and Cellular Cardiology

journal homepage: www.elsevier.com/locate/yjmcc

Original article

Distinct contractile and molecular differences between two goat models of atrial dysfunction: AV block-induced atrial dilatation and atrial fibrillation

Maura Greiser [a,*,1], Hans-Ruprecht Neuberger [a,b,1], Erik Harks [a], Ali El-Armouche [e], Peter Boknik [d], Sunniva de Haan [a], Fons Verheyen [c], Sander Verheule, Wilhelm Schmitz [d], Ursula Ravens, Stanley Nattel [g], Maurits A. Allessie [a], Dobromir Dobrev [f,2], Ulrich Schotten [a,f,2]

[a] Department of Physiology, University Maastricht, PO Box 616, 6200 MD Maastricht, The Netherlands
[b] Klinik für Innere Medizin III, Universität des Saarlandes, Homburg/Saar, Germany
[c] Department of Molecular Cell Biology, University Maastricht, Maastricht, The Netherlands
[d] Department of Pharmacology and Toxicology, University of Münster, Münster, Germany
[e] Institute of Experimental and Clinical Pharmacology and Toxicology, Medical Center Hamburg-Eppendorf, Germany
[f] Department of Pharmacology and Toxicology, Dresden University of Technology, Dresden, Germany
[g] Research Center, Montreal Heart Institute and Université de Montréal, Montreal, Quebec, Canada

ARTICLE INFO

Article history:
Received 10 June 2008
Received in revised form 21 October 2008
Accepted 3 November 2008
Available online 27 November 2008

Keywords:
Atrial fibrillation
Atrial dilatation
Contractile function
Ca^{2+} handling
Atrial remodeling

ABSTRACT

Atrial dilatation is an independent risk factor for thromboembolism in patients with and without atrial fibrillation (AF). In many patients, atrial dilatation goes along with depressed contractile function of the dilated atria. While some mechanisms causing atrial contractile dysfunction in fibrillating atria have been addressed previously, the cellular and molecular mechanisms of atrial contractile remodeling in dilated atria are unknown. This study characterized in vivo atrial contractile function in a goat model of atrial dilatation and compared it to a goat model of AF. Differences in the underlying mechanisms were elucidated by studying contractile function, electrophysiology and sarcoplasmic reticulum (SR) Ca^{2+} load in atrial muscle bundles and by analyzing expression and phosphorylation levels of key Ca^{2+}-handling proteins, myofilaments and the expression and activity of their upstream regulators. In 7 chronically instrumented, awake goats atrial contractile dysfunction was monitored during 3 weeks of progressive atrial dilatation after AV-node ablation (AV block goats (AVB)). In open chest experiments atrial work index (AWI) and refractoriness were measured (10 goats with AVB, 5 goats with ten days of AF induced by repetitive atrial burst pacing (AF), 10 controls). Isometric force of contraction (FC), transmembrane action potentials (APs) and rapid cooling contractures (RCC, a measure of SR Ca^{2+} load) were studied in right atrial muscle bundles. Total and phosphorylated Ca^{2+}-handling and myofilament protein levels were quantified by Western blot. In AVB goats, atrial size increased by 18% (from 26.6±4.4 to 31.6±5.5 mm, $n=7$ $p<0.01$) while atrial fractional shortening (AFS) decreased (from 18.4±1.7 to 12.8±4.0% at 400 ms, $n=7$, $p<0.01$). In open chest experiments, AWI was reduced in AVB and in AF goats compared to controls (at 400 ms: 8.4±0.9, $n=7$, and 3.2±1.8, $n=5$, vs 18.9±5.3 mm×mmHg, $n=7$, respectively, $p<0.05$ vs control). FC of isolated right atrial muscle bundles was reduced in AVB ($n=8$) and in AF ($n=5$) goats compared to controls ($n=9$) (at 2 Hz: 2.3±0.5 and 0.7±0.2 vs 5.5±1.0 mN/mm^2, respectively, $p<0.05$). APs were shorter in AF, but unchanged in AVB goats. RCCs were reduced in AVB and AF versus control (AVB, 3.4±0.5 and AF, 4.1±1.4 vs 12.2±3.2 mN/mm^2, $p<0.05$). Protein levels of protein kinase A (PKA) phosphorylated phospholamban (PLB) were reduced in AVB ($n=8$) and AF ($n=8$) vs control ($n=7$) by 37.9±12.4% and 29.7±10.1%, respectively ($p<0.01$), whereas calmodulin-dependent protein kinase II (CaMKII) phosphorylated ryanodine channels (RyR2) were increased by 166±55% in AVB ($n=8$) and by 146±56% in AF ($n=8$) goats ($p<0.01$). PKA-phosphorylated myosin-binding protein-C and troponin-I were reduced exclusively in AVB goat atria (by 75±10% and 55±15%, respectively, $n=8$, $p<0.05$). Atrial dilatation developing during slow ventricular rhythm after complete AV block as well as AF-induced remodeling are associated with atrial contractile dysfunction. Both AVB and AF goat atria show decreased SR Ca^{2+} load, likely caused by PLB dephosphorylation and RYR2 hyperphosphorylation. While shorter APs further compromise contractility

* Corresponding author. Tel.: +31 43 3881320; fax: +31 43 3884166.
E-mail address: m.greiser@fys.unimaas.nl (M. Greiser).
[1] M.G. and H.R.N. contributed equally to this work.
[2] U.S. and D.D. share senior authorship.

doi:10.1016/j.yjmcc.2008.11.012

in AF goat atria, reduced myofilament phosphorylation may impair contractility in AVB goat atria. Thus, atrial hypocontractility appears to have distinct molecular contributors in different types of atrial remodeling.

1. Introduction

Stroke is the 3rd leading cause of death in Western countries and a major cause of long-term disability, with important socioeconomic consequences. With population aging, the stroke-related burden will continue to increase. Identification and treatment of risk factors for stroke are likely to have positive effects on stroke morbidity and mortality [1]. Of all strokes, 88% are ischemic, with cardiac thromboembolism as a frequent cause [2]. Atrial dilatation is an independent risk factor for thromboembolic cerebrovascular disease [3–5]. However, the mechanisms underlying thromboembolism in dilated atria associated with various forms of cardiac pathology are not yet clear. As atrial size increases, blood flow velocity decreases and thrombus formation may occur, increasing embolic risk. In addition, contractility may be impaired in dilated atria, representing a 'dilated atrial cardiomyopathy'. In animal models of heart failure, atrial emptying function is reduced [6] and in patients subjected to ventricular demand pacing (VVI) loss of atrioventricular synchrony increases LA diameter while markers of atrial contractility decrease [7]. Whether loss of atrial contractility in dilated atria is due to changes in preload or due to an intrinsic depression of force of contraction of the atrial myocardium is unknown. Cellular mechanisms underlying atrial contractile dysfunction in dilated atria are largely unexplored, while some aspects of the mechanisms underlying contractile dysfunction of the atria associated with atrial fibrillation (AF) have been characterized. During the first days of AF, atrial contractile dysfunction appears to be related to a reduction of the Ca^{2+} inward current ($I_{Ca,L}$), resulting in action potential (AP) shortening [8]. In a later stage, upregulation of the Na^{+}/Ca^{2+}-exchanger [9], impaired myofibril energetics [10] and impaired Ca^{2+} release from the sarcoplasmic reticulum (SR) [11] also play a role. While myolysis occurs, its contribution to loss of contractility is apparently limited [12].

This study investigated whether atrial dilatation in goats with a slow ventricular rate due to chronic AV block (AVB goats) is associated with decreased atrial contractile function independent of atrial preload (intrinsic myocyte remodeling). Since shortening of the action potential was reported in some [13] but not all animal models of atrial dilatation [14,15] we tested the hypothesis that the mechanisms underlying atrial contractile abnormalities differ in atrial dilatation developing after complete AV block versus AF-induced atrial remodeling. In order to assess intrinsic muscle remodeling, contractile function and SR Ca^{2+} loading were studied in atrial muscle bundles. Expression and phosphorylation levels of key Ca^{2+}-handling proteins, myofilaments and important regulators (PKA, CaMKII, phosphatases) were evaluated in atrial tissue to identify specific molecular determinants of contractile dysfunction in these models.

2. Methods

2.1. Animal models and experimental protocols

Forty-two female white Dutch milk goats (age range: 1–2 years) weighing 48±3 kg were used. Animal handling was performed according to the European directive on laboratory animals (86/609/EEC), the study protocol was approved by the ethical committee for animal studies at the faculty of Medicine at the University of Maastricht (Dierexperimenten Commissie). The investigation conformed with the Guide for the Care and Use of Laboratory Animals published by the US National Institutes of Health (NIH Publication No. 85-23, revised 1996).

Two series of goats were studied. In series 1, changes in atrial contractility associated with 3 weeks of atrial dilatation after induction of chronic AV block were assessed in chronically instrumented awake goats (AVB goats). Since the time course of atrial contractile dysfunction is already well-characterized in AF-induced remodeling [8] we did not include AF goats in this series. Series 2 evaluated the mechanisms of atrial contractile dysfunction in AVB goat atria and compared them to those induced by AF. Three groups of animals were studied: Series 2a: goats with atrial dilatation after induction of chronic AV block (=AVB), series 2b: goats with AF induced by repetitive burst pacing (=AF) and series 2c: control goats (control). In series 2, open chest experiments were performed to assess atrial contractile function in vivo and tissue was harvested for experiments in atrial muscle bundles, electron microscopy and biochemistry.

2.2. Loss of atrial contractility in awake goats with AV block-induced atrial dilatation (series 1)

Seven goats were instrumented under general anesthesia (thiopental 10–15 mg/kg i.v.; halothane 1% and a 1:2 mixture of O_2 and N_2O) with two right atrial (RA) leads and one ventricular pacing lead before inducing complete AV block by His bundle ablation, as described previously [14]. Ultrasound crystals mounted at the tip of the atrial leads were used to measure atrial diameter as a surrogate parameter for RA size (Fig. 1A). A VVI pacemaker with an intervention rate of 45 bpm was connected to the ventricular lead. RA and pulmonary wedge pressures were measured with a Swan–Ganz catheter. After recovery, RA size, atrial fractional shortening (AFS; Fig. 1), and atrial effective refractory period (AERP) were measured during RA pacing at 400 and 300 ms cycle length in awake animals. Three weeks later, atrial contractile function and refractoriness were determined again. RA and pulmonary wedge pressures were recorded under general anesthesia.

2.3. Mechanisms of atrial contractile dysfunction in AVB and AF goats (series 2)

In 14 goats (series 2a), chronic AV block was induced and VVI pacing (45 bpm) was initiated as described above. Four weeks later, the chest was opened under general anesthesia and RA pressure-diameter-loops were recorded using sonomicrometer crystals and a tip pressure transducer as described previously [16]. Atrial diameter, pressure and refractoriness were recorded during RA pacing at varying cycle lengths. Identical measurements were performed in 7 goats with 10 days of AF induced by repetitive burst pacing with an Itrel pacemaker [17] (series 2b) and in 11 control goats (series 2c). After completion of measurements, the atria were excised and transferred into cold (+5 °C) Ca^{2+}-free Tyrode's solution. The anteroposterior and craniocaudal dimensions of RA and LA free walls and their weight were determined. Part of the tissue was stored in liquid nitrogen (biochemistry) or 3% glutaraldehyde (electron microscopy).

2.4. Muscle bundle experiments

Right atrial muscle bundles of less than 0.8 mm diameter were prepared and isometric force of contraction (FC) was measured between 0.5 and 3 Hz as described previously [12]. The SR Ca^{2+} load was assessed as amplitude of contractures after rapid cooling (RCCs) of muscle bundles from 37 °C to 1 °C as described elsewhere [18]. Briefly, preparations were rapidly (within 1 s) transferred from a 37 °C to a

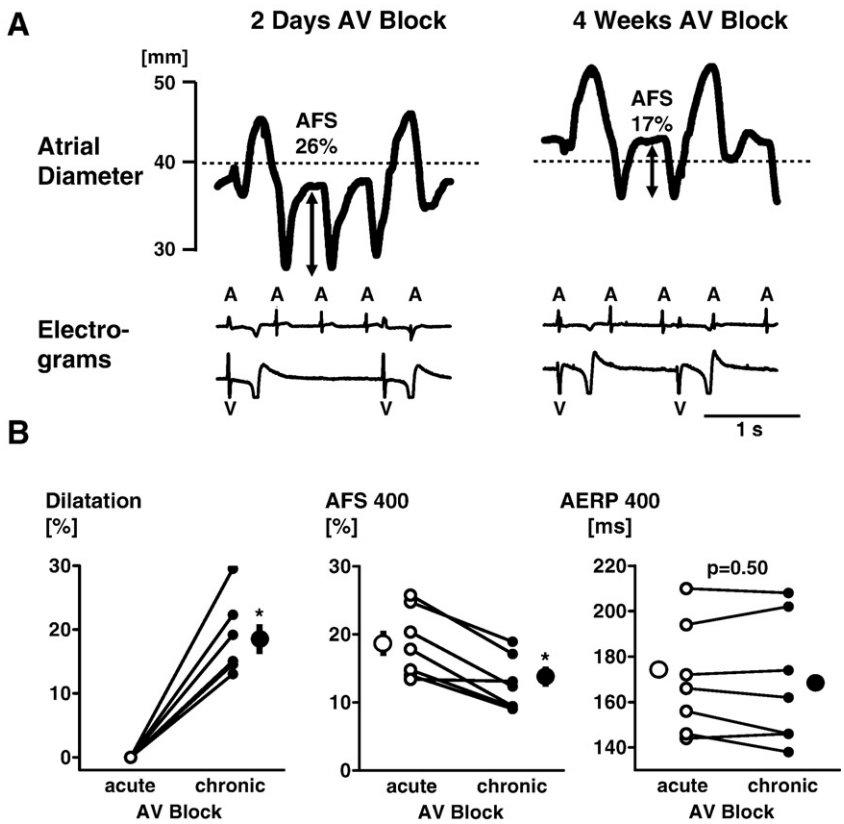

Fig. 1. (A) RA diameter measured with transvenously implanted ultrasound crystals (upper tracings) together with RA and ventricular electrograms during acute and chronic AV block. Note the isolated atrial contractions during the long diastolic pause. The last atrial contraction before a ventricular activation was used to determine atrial fractional shortening (AFS). (B) Effect of 3 weeks of AV block on atrial diameter, fractional shortening and AERP during slow atrial pacing at 400 ms cycle length. $n=7$ goats, *: $p<0.05$ vs control.

0 °C bathing solution, while carefully maintaining preparation length. Muscle bundles were not stimulated during cooling. Transmembrane action potentials (APs) were recorded during field stimulation with microelectrodes (tip resistance 30–40 MΩ, filled with 3 M KCl) to determine resting membrane potential, AP amplitude and AP duration (APD).

2.5. Morphology and morphometry

Morphometry was performed as described previously [17]. Small right atrial blocks (4 mm^3) were fixed in 3% glutaraldehyde (pH 7.4 with 90 mM KH_2PO_4), postfixed in 1% osmium tetroxide in Na-cacodylate buffer, dehydrated in graded series of ethanol and routinely embedded in epoxy resin. Ultrathin sections were cut from transversely sectioned cardiomyocytes, counterstained with uranium acetate and lead citrate, and examined in a Philips CM100 electron microscope. For morphometry, electron microscope photographs were obtained at a magnification of 1650× and the surface area of transversely-sectioned cells and cytoplasmic structures were quantified by the point-counting method (20×26 point-counting grid).

2.6. Western blot, kinase and phosphatase activity measurements

RA homogenates were obtained from frozen tissue and protein concentrations were determined with Amido-Black 10B [19]. Proteins were fractionated on SDS-polyacrylamide gels and transferred to nitrocellulose membranes (BioTrace®NT, Life Sciences). Western blotting was performed with primary antibodies to calsequestrin (CSQ, 1:2500; Dianova), alpha$_{1C}$ Ca^{2+}-channel subunit (custom-made affinity-purified rabbit polyclonal antibody, 1:100; kind gift from Dr. H. Haase, Max Delbrück Center for Molecular Medicine, Berlin), troponin-I (Tn-I, 1:30,000; Chemicon), Kv4.2 subunit of transient outward K^+-current I_{to} (1:1000; Upstate Biotechnology), G-protein-coupled inwardly rectifying K^+-channel subunit-4 (GIRK4, 1:200; Santa Cruz), Ser23/24-phosphorylated Tn-I (1:5000; Cell Signaling), troponin-C (monoclonal; 1:1000; Fitzgerald), SR Ca^{2+}-ATPase (SERCA2a, 1:2000; Santa Cruz), Thr287-phosphorylated Ca^{2+}/calmodulin protein kinase II (CaMKIIδ, 1:5000; Promega), catalytic protein kinase A (PKAc, 1:1000; BD Transduction Laboratories), regulatory PKA IIα (1:500; Santa Cruz), total, Ser16- and Thr17-phosphorylated phospholamban (PLB, all 1:5000; Badrilla), protein phosphatase 1α (PP1α, 1:500; Biomol), protein phosphatase 2A (PP2A, 1:2000, affinity purified; Upstate Biotechnology), atrial natriuretic peptide (ANP, 1:10,000; Acris Antibodies GmbH), total myosin-binding protein C (MyBP-C, 1:5000; kind gift from Dr. Wolfgang Linke, University of Münster), and Ser282-phosphorylated MyBP-C (1:1000; Eurogentec), total ryanodine receptor (RYR2), Ser2809- and Ser2815-phosphorylated RYR2 (1:5000, 1:5000 and 1:2500, respectively; kind gifts from Dr. Andrew Marks, Columbia University), as previously described [20]. Detection was obtained with suitable secondary antibodies and protein bands were visualized by electrochemoluminescence reagents (Pierce) and Hyperfilm-ECL (Amersham). Films were evaluated densitometrically with Phoretix 1D software (Biostep). Kinase and phosphatase activities were measured in atrial homogenates as previously described [21]. Cyclic AMP (2 μmol/l) was used to maximally stimulate PKA, okadaic acid (3 nmol/l) was used to differentiate between PP1 and PP2A activities [21].

2.7. Statistics

Results are given as mean±SEM. Student's *t*-test was used to evaluate differences between AV block and control. Multiple groups were compared by analysis of variance (one-way ANOVA). $P<0.05$ was considered statistically significant.

3. Results

3.1. Atrial size, contractile function and refractoriness in atria of awake AVB goats

The RA diameter in awake goats 2 days after His bundle ablation was 26.6±4.4 mm and increased to 31.6±5.5 mm after 3 weeks of AV block (+18.4±2.2%, $p<0.01$; Fig. 1B). AFS had decreased by 20–30% (AFS_{400} from 18.4±1.7 to 12.8±4.0%, $p<0.01$; AFS_{300} from 15.4±1.9 to 11.9±1.5%, $p<0.05$). $AERP_{400}$ and $AERP_{300}$ did not change significantly (from 170±9 to 168±11 ms; 163±9 to 161±8 ms, respectively). Immediately after His bundle ablation, RA pressure was 11.9±1.5 mmHg and did not change throughout 3 weeks of AV block (9.2±1.0 mmHg, $p=0.53$), indicating comparable preloads during AFS and AERP measurements. Wedge pressures also remained unchanged (acutely after His bundle ablation 9.7±2.1 mmHg vs. 11.7±1.1 mmHg 3 weeks later, $p=0.66$), indicating stable left-ventricular pump function.

3.2. Atrial size, contractile function and refractoriness in open chest experiments

In AVB goats, both atria were significantly enlarged compared to controls. The antero-posterior and craniocaudal dimensions of the dilated RA were 6.1±0.2 and 3.3±0.1 cm vs. 4.9±0.3 and 2.5±0.1 cm in control animals ($p<0.01$), corresponding to an increase in atrial surface area of ~64%. Similar results were obtained for the LA (5.4±0.1 and 4.3±0.2 cm vs. 4.1±0.2 and 3.1±0.1 cm, $p<0.001$). After 4 weeks of AV block, the RA weighed 0.35±0.06 vs. 0.16±0.01 g/kgBW in control ($p=0.02$) and the LA weighed 0.26±0.02 vs. 0.12±0.01 g/kgBW ($p=0.002$), respectively.

Fig. 2A shows RA pressure-diameter-loops from a control (left), an AVB (mid panel) and an AF goat (right) recorded during atrial pacing with a cycle length of 400 ms. The hatched area enclosed by the loop represents AWI [8]. Both in AVB and AF goat atria the loop was almost closed, indicating impaired contractility and mainly passive atrial movement. AWI was significantly reduced in AVB goats at cycle lengths of 300 and 400 ms (e.g. AWI_{400}: 8.4±0.9 vs. 18.9±5.3 mm×mmHg in control animals, $p<0.05$). In AF, loss of atrial contractility was more pronounced (AWI_{400}: 3.2±1.8 mm×mmHg, $p<0.05$ vs. control, Fig. 2B. In AVB goats, the right atrial ERP tended to be longer than in controls (reaching significance only at 450 ms: $AERP_{450}$: 155±10 vs. 125±6 ms, $p<0.05$), while ERPs were shortened in AF at all cycle lengths (Fig. 2C).

3.3. Contractile function, action potentials and indices of SR Ca^{2+} content in isolated muscle bundles

Transmembrane APs did not show significant differences in AP duration (APD) at 70% (APD_{70}) or 90% repolarization (APD_{90}) between control and AVB goats. Both groups showed positive APD rate adaptation. In AF goats, APD_{70} and APD_{90} were significantly shortened at cycle lengths >400 ms (APD_{70}) or >333 ms (APD_{90}) and rate adaptation was blunted (Figs. 3A, B). There were no differences in early repolarization (APD_{30}), resting membrane potential, and AP amplitude between the three groups. Fig. 3C shows the data at 1 Hz. FC was equally reduced at all stimulation rates by ~50% in AVB and ~80% in AF (e.g. at 2 Hz: 5.5±1.0 mN/mm^2 in control, 2.3±0.5 mN/mm^2 in AVB, and 0.7±0.2 mN/mm^2 in AF, $p<0.05$; Fig. 3D. In all three groups, the force-frequency relation was negative. Diastolic function at a physiological stimulation frequency (time to 90% relaxation, 2.5 Hz) was not different in AVB and AF goats compared to controls (113±5.3, 114±9.5 and 109±5.4 ms, respectively, $p=0.86$). At a stimulation rate of 1 Hz, SR Ca^{2+} content (based on RCCs) tended to be lower in AVB (4.3±1.1 mN/mm^2) and AF goats (4.9±0.7 mN/mm^2) compared to controls (6.4±1.1 mN/mm^2, $p=0.23$). In control goats, increasing the stimulation rate to a physiologic frequency (2.5 Hz) increased RCCs

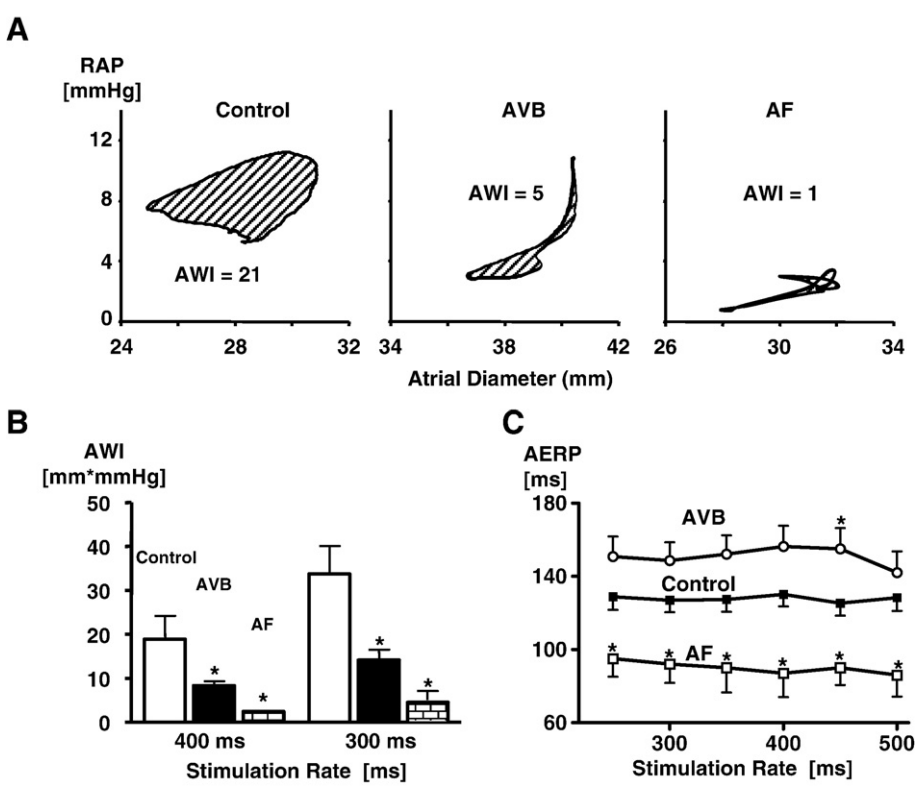

Fig. 2. (A) Pressure-diameter loops in anaesthetized control goats, after 4 weeks of AV block, and after 10 days of AF. The area enclosed by the loop provides the atrial work index (AWI, mm mmHg). (B, C) Right atrial AWI and AERP during open chest experiments in control goats ($n=5$–7), goats with 4 weeks of AV block ($n=7$–10), and AF goats ($n=5$). *: $p<0.05$ vs control.

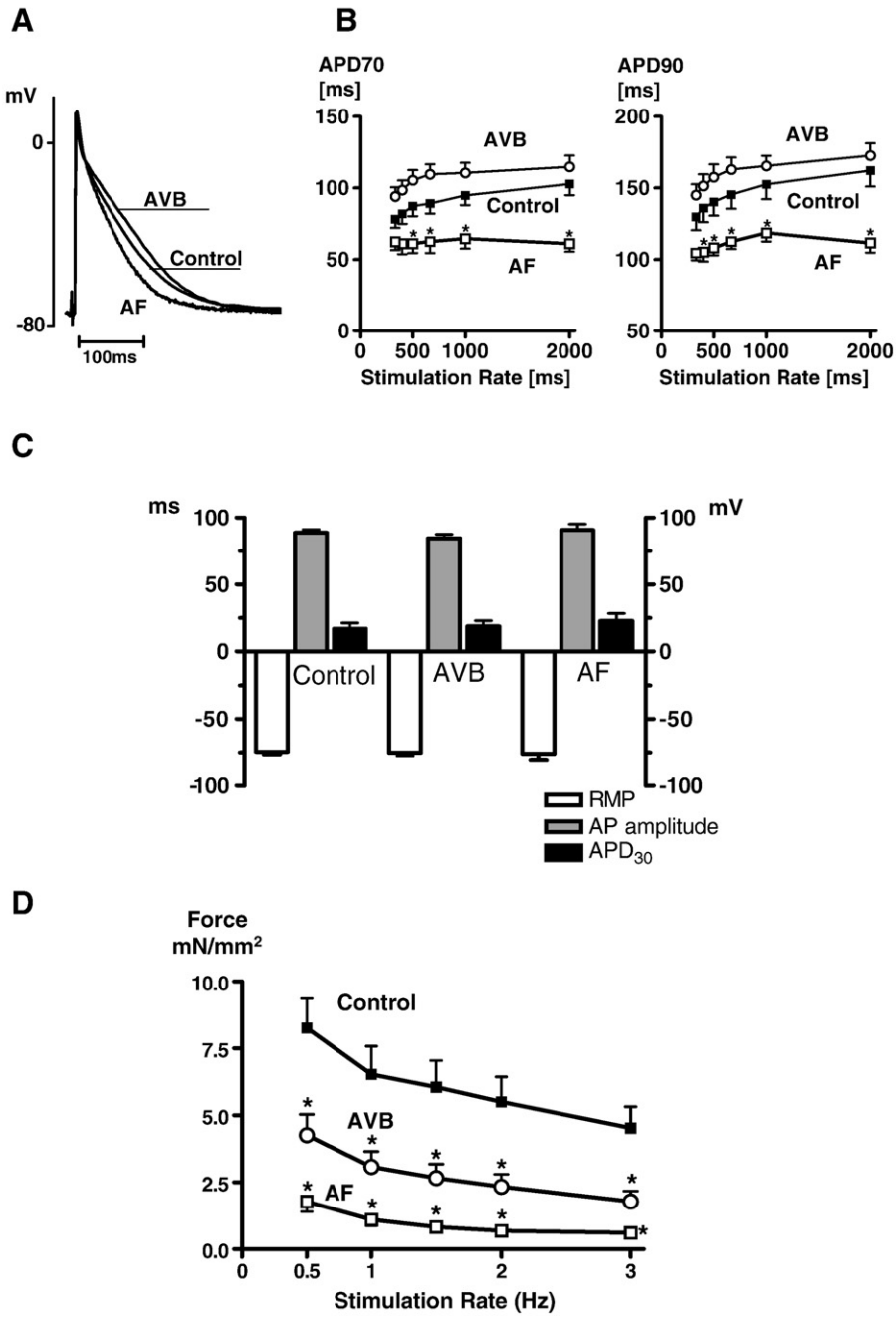

Fig. 3. (A) Representative transmembrane APs (left) and average APD_{70} and APD_{90} in 15 bundles from 9 control goats, 16 bundles from 8 AVB goats and 7 bundles from 5 AF goats (right). (B) Resting membrane potential (RMP), AP amplitude and APD_{30} in muscle bundles from control, AVB and AF goats at 1 Hz. (C) Contractile force of isolated muscle bundles was ~50% lower in AVB (22 bundles from 10 goats) and further reduced in AF (by ~75% in 10 bundles from 5 goats) compared to control (20 bundles from 10 goats). The effect of rate on force was similar in all groups. * $p<0.05$, vs. control.

nearly two-fold (12.2±3.2 mN/mm^2, $p<0.05$; Fig. 4). However, this frequency-dependent increase in RCC amplitude was lost in both AVB (3.4±0.5 mN/mm^2) and AF (4.4±0.7 mN/mm^2) goats suggesting that at physiological frequencies SR Ca^{2+} load is significantly decreased.

3.4. Electron microscopy

Electron microscopy revealed moderate changes in atrial myocyte ultra-structure in both AVB and AF goats (Fig. 5). The content of contractile material (sarcomeres) was reduced from 50±1% in control to 42±1% in AVB goats (−17.2%, $p<0.05$) and to 40±1% in AF goats (−21.0%, $p<0.05$). Pronounced accumulation of glycogen was present at the perinuclear region in AVB (34±1% vs. 21±1% in control, $p<0.05$) and AF (39±1% vs. 21±1%, $p<0.05$) goats. Average surface areas of nuclei, mitochondria, and other membrane structures were unaltered.

3.5. Ion channel, Ca^{2+}-handling and myofilament proteins

In Western blot analysis, protein-band intensities were normalized to those of CSQ on the same blots (mean CSQ intensities were similar in all groups; not shown). Protein levels of α_{1C}, Kv4.2 and GIRK4 channel subunits were comparable in all groups (Supplemental Fig. 1). ANP expression was increased by 52% in AVB and by 38% in AF goats suggesting development of hypertrophy in both models (Supplemental Fig. 2).

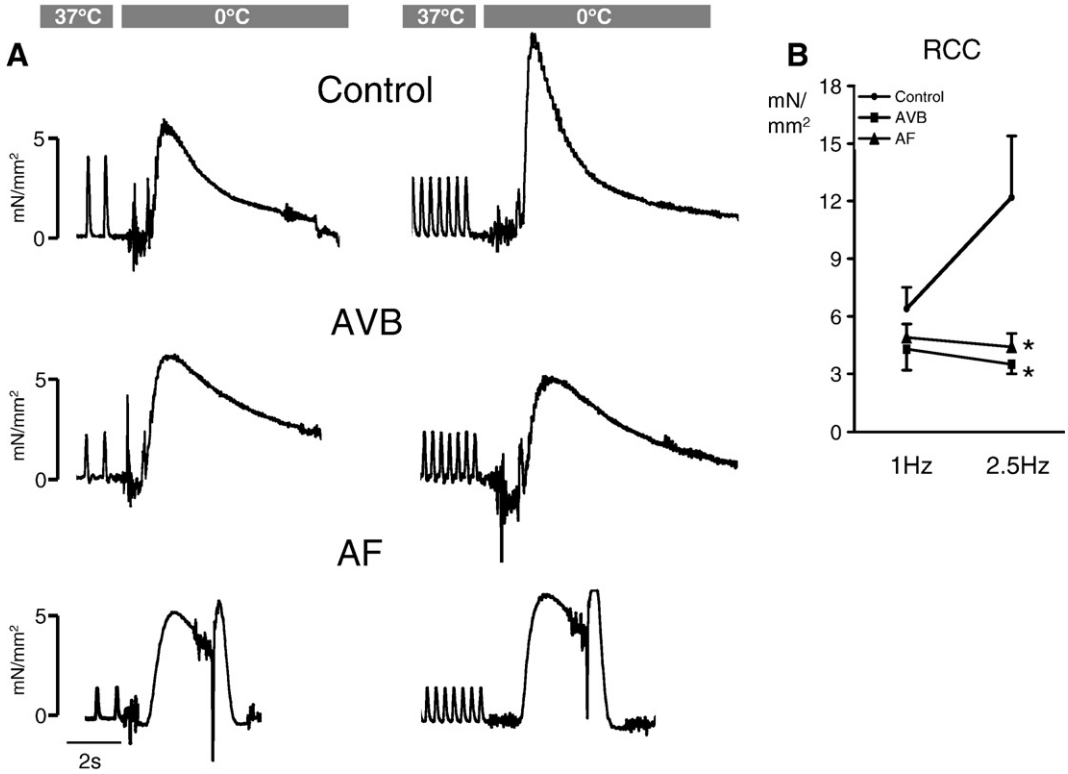

Fig. 4. (A) Rapid cooling contractures (RCCs) at 1 and 2.5 Hz. (B) Average RCCs in control (10 bundles from 7 goats), AVB (11 bundles from 6 goats), and AF goats (11 bundles from 4 animals). *: $p<0.05$ versus control.

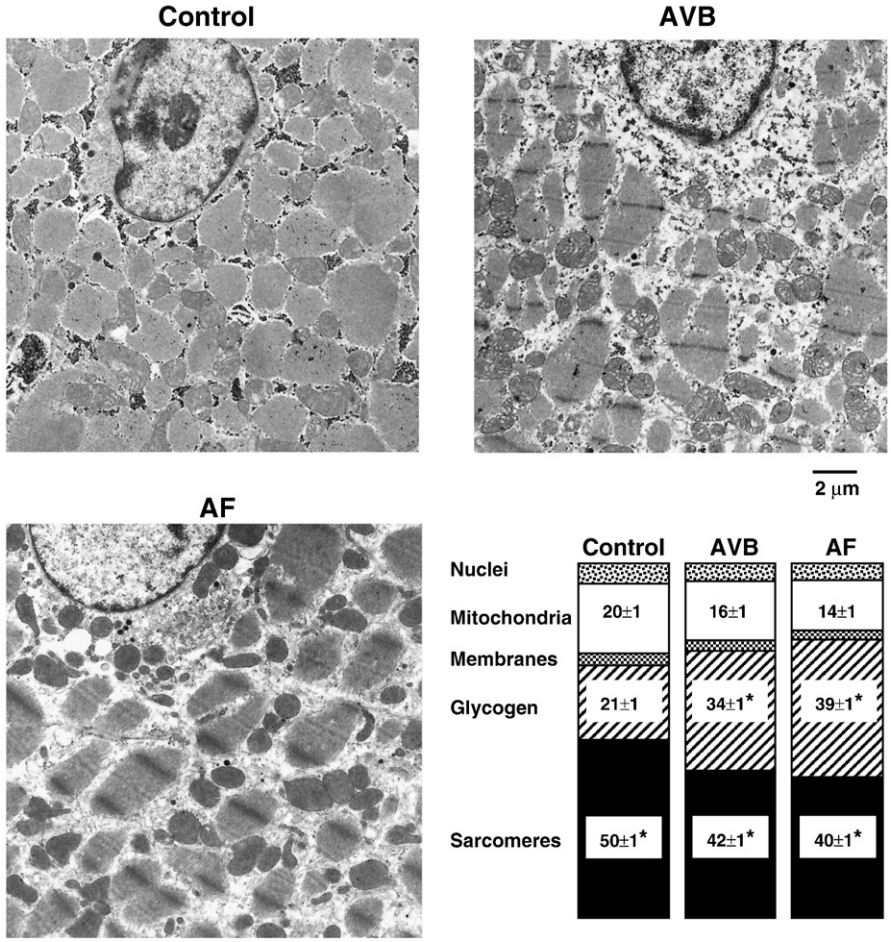

Fig. 5. Electron microscopy of atrial myocytes from control (118 cells, 6 goats), AVB (99 cells, 7 goats), and AF goats (171 cells, 4 goats). *: $p<0.05$ versus control.

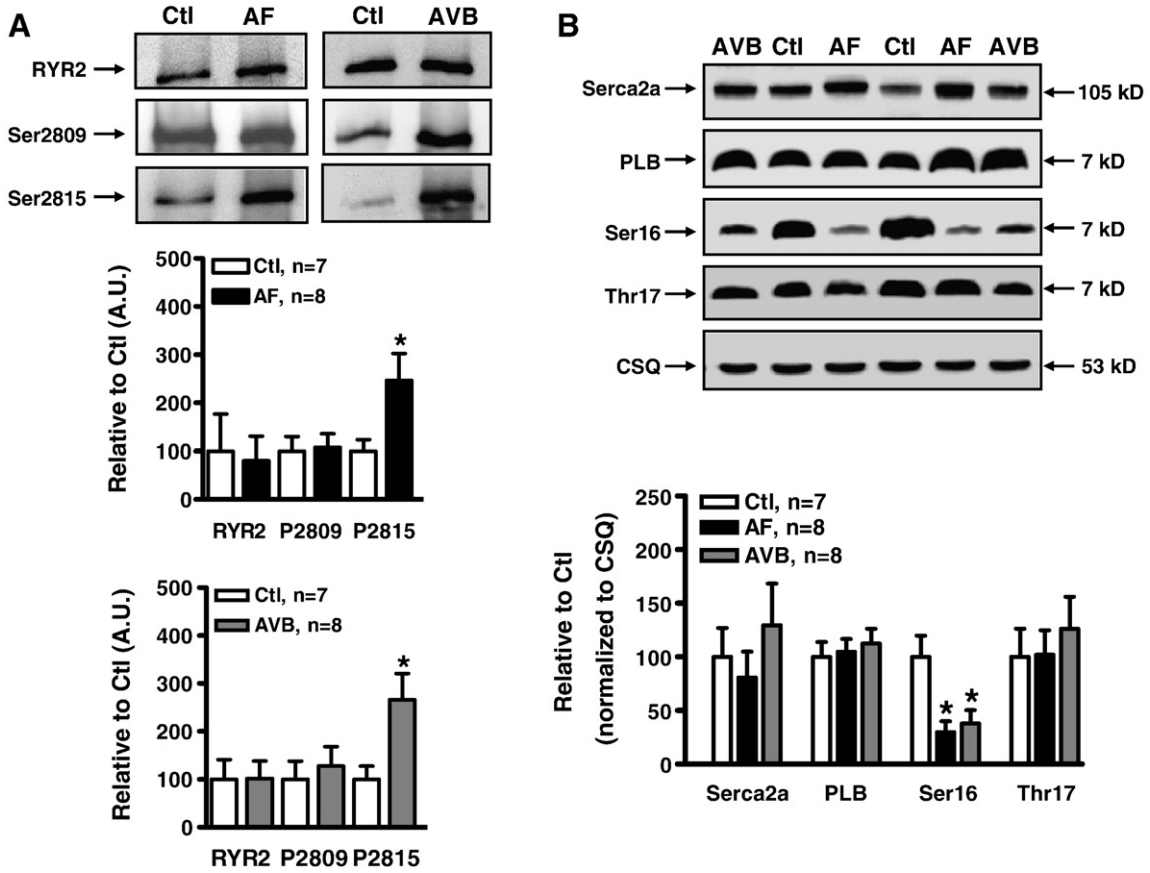

Fig. 6. Total and phosphorylated RyR2 and PLB proteins in control, AF and AVB atria. (A) Top: A gel showing representative examples of total, Ser2809-P and Ser2815-P RYR2. Bottom: band intensities relative to control. (B) Top: A gel showing representative examples of Serca2a, total PLB, Ser16-P PLB and Thr17-P PLB, and calsequestrin (CSQ). Bottom: band intensities normalized to CSQ, relative to control. *: $p<0.05$ versus control.

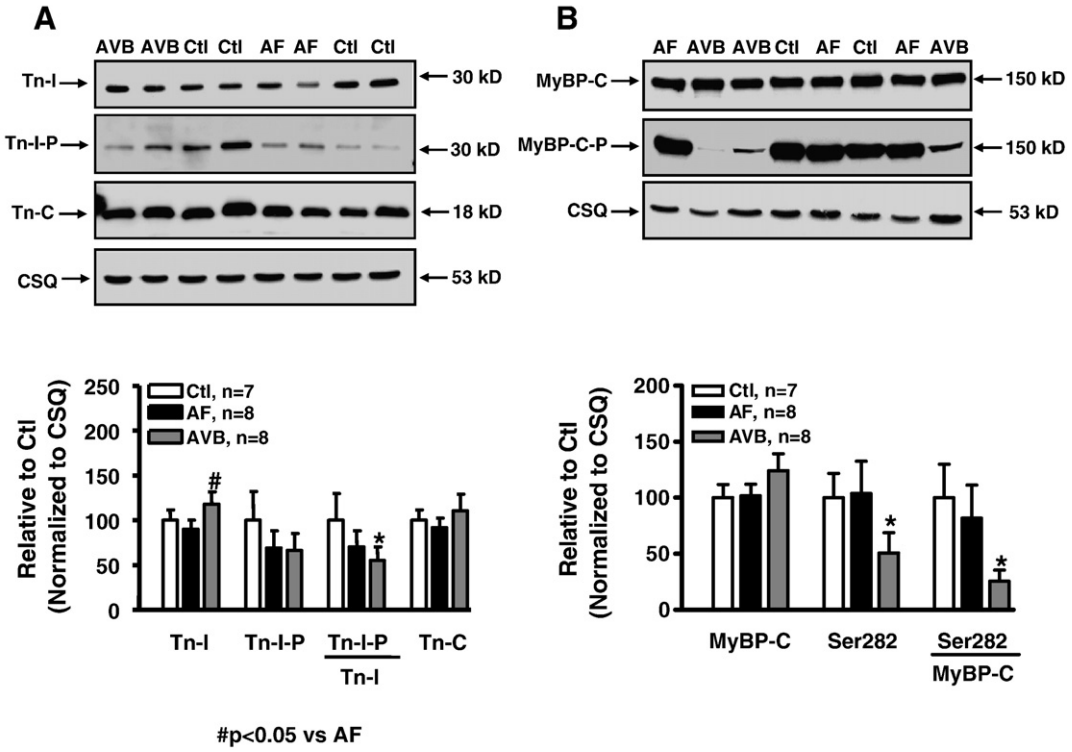

Fig. 7. Myofilament protein expression (total and phosphorylated forms) in control, AF and AVB. (A) Top: A gel showing representative examples of total and Ser23/24-P Tn-I, and calsequestrin (CSQ). Bottom: protein band intensities normalized to CSQ, relative to control. (B) Top: A gel showing representative examples of total and Ser282-P MyBP-C, and CSQ. Bottom: Protein band intensities normalized to CSQ, relative to control. *: $p<0.05$ versus corresponding control.

Total and PKA-phosphorylated RyR2 at Ser2809 were unchanged in AVB and AF goats, whereas CaMKII-phosphorylated RyR2 at Ser2815 was significantly increased, by ~166% and 146% respectively (Fig. 6A). The protein abundances of Serca2a and PLB were similar in all groups (Fig. 6B). Ser16-phosphorylated PLB was 70% and 62% lower in AF and AVB goats, respectively, with no corresponding alterations in Thr17-phosphorylated PLB. The same was true for Ser16-PLB or Thr17-PLB to total PLB ratios (Fig. 6B).

Total Tn-I expression was increased in AVB goats (vs AF, $p<0.05$, Fig. 7A) while total expression of troponin C was similar in all groups (Fig. 7A). PKA-phosphorylated (Ser23/24) to total Tn-I ratio was lower in AVB goats, but unchanged in AF, suggesting potentially increased myofibrillar Ca^{2+} sensitivity exclusively in AVB goats. Total thick myofilament MyBP-C was unchanged, whereas PKA-phosphorylated MyBP-C at Ser282 was decreased by 75% in AVB goats only (Fig. 7A).

Since PP1 and PP2A activities are increased in AF patients [20,22] we hypothesized that an altered phosphatase activity may contribute to the reduced PKA-phosphorylation of PLB in AF and of PLB, Tn-I and MyBP-C in AVB. We found similar protein abundances of PP1 and PP2A and unchanged total PP1 and PP2A activities in AF and AVB goats, suggesting potential abnormalities of CaMKII and/or PKA function (Supplemental Fig. 3). Accordingly, protein abundance of the regulatory PKA_{RII} subunit, but not of PKAc, was decreased by 25% and 45% in AF and AVB goats respectively (Fig. 8C) suggesting potentially limited targeting of PKAc to substrates in both settings. PKA activity under basal (absence of cAMP) and cAMP-stimulated (2 μM) conditions was decreased in AF by 57% and by 36%, respectively, and tended to be reduced under both conditions also in AV block goats (Fig. 8B). Expression of the activated cytosolic CaMKIIδ isoform (autophosphorylated at Thr287) was increased by 262% and 95% in AVB and AF, respectively, whereas the nuclear CaMKIIδ isoform was enhanced by 123% in AVB only (Fig. 8C). Determination of total CaMKIIδ was not possible because our total CaMKIIδ antibody was of goat origin.

4. Discussion

This study shows that atrial dilatation in goats with complete AV block is associated with a pronounced reduction of intrinsic atrial contractility. The mechanisms underlying atrial contractile dysfunction in chronic AV block goats differ from those causing atrial contractile dysfunction in AF-induced remodeling. AF impairs atrial contractility by APD shortening due to a reduction of $I_{Ca,L}$ [23,24] and a decrease in SR Ca^{2+} load. In AVB goats, atrial APD shortening does not occur and contractile dysfunction probably involves decreased SR Ca^{2+} load and 'atrial myofibrillar remodeling', likely related to a reduction of PKA-phosphorylated MyBP-C and Tn-I. These results elucidate molecular mechanisms of adverse contractile remodeling in dilated and fibrillating atria that may help to identify potential targets to treat atrial contractile dysfunction.

4.1. Atrial dilatation and contractile dysfunction

In animal models, only moderate reductions of $I_{Ca,L}$ have been reported in atrial dilatation due to heart failure [25] or aorto-pulmonary artery shunt [13]. We have reported that 3 weeks of AV

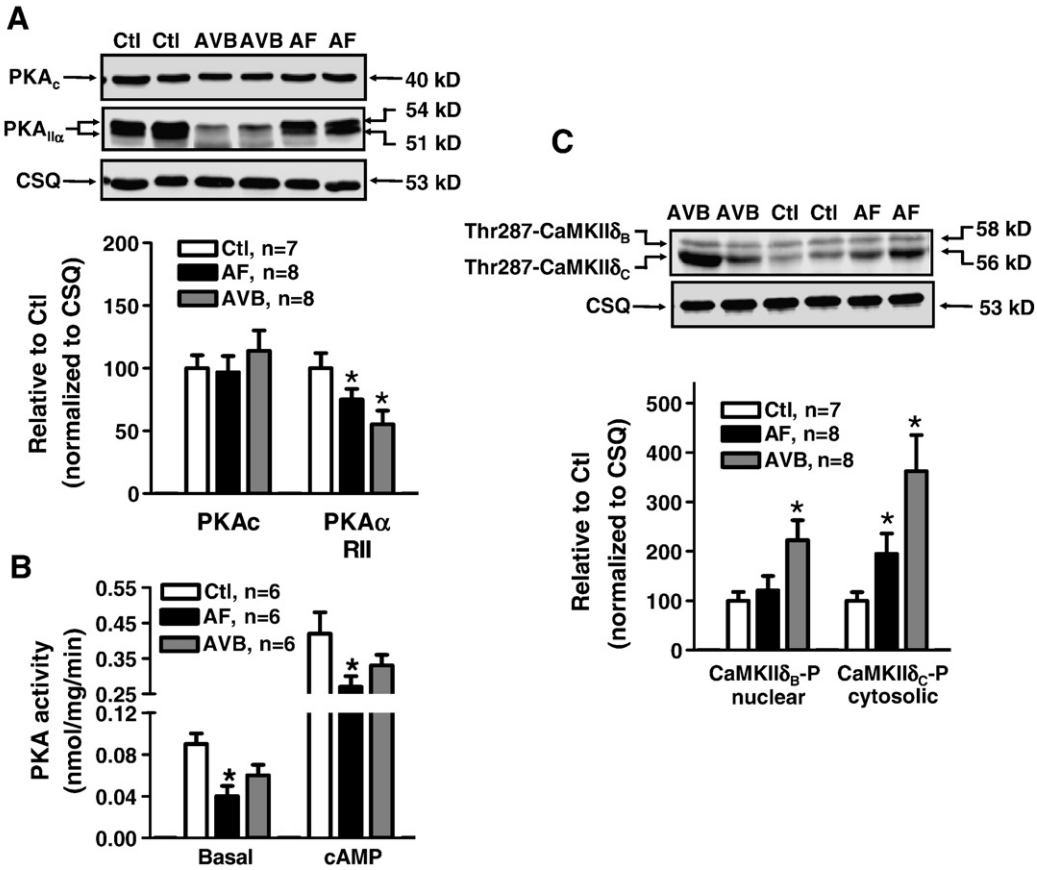

Fig. 8. Protein kinase A kinase activity and corresponding protein expression in control, AF and AVB atria. (A) Protein levels of catalytic and regulatory PKA subunits in control, AF and AVB atria. Top: A gel showing representative examples of PKA_C, $PKA_{II\alpha}$ and CSQ. The $PKA_{II\alpha}$ antibody recognized two bands at 51 and 54 kD, respectively. Quantification is based on the sum of the two bands. (B) Protein kinase A activity measured under basal (no cAMP) and stimulated (2 μM cAMP) conditions in homogenates of control, AF and AVB goat atria. (C) Autophosphorylated (activated) CaMKIIδ in control, AF and AVB atria. Top: A gel showing representative examples of Thr287-CaMKII and CSQ. Top band (58 kD) represents $CaMKII\delta_B$, bottom band (56 kD) corresponds to $CaMKII\delta_C$. Bottom: Protein band intensities normalized to CSQ and relative to control. *: $p<0.05$ versus corresponding control.

block and slow idioventricular rhythm in awake goats induce pronounced right and left atrial dilatation [14]. This was accompanied by a ~30% decrease in AFS. Atrial pressure remained stable during three weeks after His bundle ablation, indicating that changes in preload cannot account for impaired atrial contractility. ANP expression was increased in both AVB and AF in line with the development of hypertrophy in these models. Enhanced ANP may contribute to atrial amyloidosis [26] that impairs atrial conduction and/or contraction. In AVB, isometric FC was ~50% lower, whereas atrial myocyte sarcomere content was decreased by ~17% only. Recently we showed an evenly reduced extracellular matrix content and a slightly increased cardiomyocyte surface area (by ~5%) [14]. Thus, the relative reduction in contractile material equals ~11%, indicating small contribution of myolysis to hypocontractility. In AF goats, sarcomere content was decreased by ~21% while FC was reduced by ~80%. In this model significant changes of extracellular matrix have not been detected [27].

4.2. Mechanisms of atrial contractile dysfunction in AVB versus AF atria

During the first days of AF, shortening of atrial refractoriness (electrical remodeling) and the decline of atrial contractile function follow the same time course [8], suggesting that $I_{Ca,L}$ reduction is a major contributor to contractile dysfunction in AF. Channel subunits of α_{1C} (for $I_{Ca,L}$), Kv4.2 (for I_{to}), and GIRK4 (for $I_{K,ACh}$) were unchanged in all groups which together with unaltered resting membrane potential and APD_{30} suggests post-translational ion channel modifications (e.g. kinase/phosphatase imbalances) as the potential underlying mechanism for reduced $I_{Ca,L}$. In AVB goats, APD and refractoriness were unchanged, indicating preserved $I_{Ca,L}$ function and thus distinct cellular mechanisms compared to AF.

The estimation of SR Ca^{2+} loading by RCCs showed a strong frequency-dependent reduction of SR Ca^{2+} load of ~70% in both AVB and AF. This identifies a reduced SR Ca^{2+} loading capacity as an important cause of impaired contractility in both conditions at physiological frequencies, as fractional Ca^{2+} release (and gain) decrease dramatically at ~50% reduction in SR Ca^{2+} content [28]. In the failing human ventricle, reduced SR Ca^{2+} loading is the consequence of decreased SR Ca^{2+} uptake and increased SR Ca^{2+} leak via RYR2 release [29]. Here, we detected a ~60% dephosphorylation of PLB in AVB and AF, suggesting reduced activity of Serca2a (because of enhanced inhibition via dephosphorylated PLB) and consequently decreased Ca^{2+} sequestration into the SR. Under these conditions relatively more Ca^{2+} will be extruded into the extracellular space via the Na^+/Ca^{2+} exchanger, which will further deplete SR Ca^{2+} content. An increased diastolic leak of Ca^{2+} through CaMKII-hyperphosphorylated RYR2 could also contribute to the reduced SR Ca^{2+} load in AVB and AF and could be reconciled with the reduction of SR Ca^{2+} load exclusively at higher frequencies due to the stimulation rate dependent activation of CaMKII. Moreover, we identified an altered regulation of contractile proteins exclusively in AVB goats. PKA-phosphorylation of MyBP-C at Ser-282 was reduced by ~75%. Since PKA-phosphorylation of MyBP-C determines maximum force development, stretch-dependent augmentation of force-generation, and cross-bridge cycling kinetics, [30] reduced PKA-phosphorylation of MyBP-C might contribute to contractile dysfunction in AVB goats.

Phosphorylation of Tn-I decreases myofibrillar Ca^{2+} sensitivity. In AVB goats we found a 46% decrease of PKA phosphorylated Tn-I (Ser23/24) together with an increase in total Tn-I (vs AF). However, the functional consequences of these Tn-I alterations are unclear since the diastolic function of the isolated muscle bundles was preserved. Reduced PKA-phosphorylation of Tn-I and MyBP-C is consistent with data in human and canine models of cardiomyopathy [31] and with reduced PKA-phosphorylation of MyBP-C in patients with chronic AF [20]. Although a distinct pattern of myofilament remodeling may contribute to contractile dysfunction in AVB versus AF goats, systematic force measurements in skinned fibers are required to directly demonstrate contribution of intrinsic myofilament remodeling to hypocontractility of AVB and/or AF goats.

Reduced PKA activity in AF and a trend towards reduced PKA activity in AVB together with a reduced expression of the PKA_{RII} subunit that controls PKAc targeting to cellular microdomains suggest that limited local availability of catalytic PKAc may account for the decreased PKA-phosphorylation of PLB, MyBP-C, and Tn-I in AVB and of PLB in AF goats. Although enhanced activity of PP1 and PP2A contributes to reduced phosphorylation of MyBP-C in human chronic AF, atrial phosphatase expression and activity are unchanged in AF and AVB goats. This indicates that during the early stages of remodeling reduced PKA-mediated substrate phosphorylation, rather than increased PP1- and PP2A-mediated dephosphorylation, is the most likely mechanism of the phosphorylation changes we observed. Similarly, enhanced CaMKII-autophosphorylation (and activation) could explain the increased fractional CaMKII-phosphorylation of RYR2. However, changes in ventricular kinase and phosphatase expression/activity within the RYR2 complex do not necessarily follow global changes in these enzymes [32] suggesting local control in subcellular compartments and this may explain why CaMKII phosphorylation of PLB at Thr17 was lower in AVB and AF goats. Thus, it is very likely that the distinct changes in RYR2, PLB, MyBP-C and Tn-I phosphorylation in AVB and AF goats are a consequence of local kinase/phosphatase regulation within the macromolecular protein complexes. The phenotype of varying changes in phosphorylation of different proteins phosphorylated by a common enzyme seems to be a general feature of stress responses in cardiac myocytes under broad ranges of conditions. The underlying basis of this phenomenon, which has been observed in many studies, has yet to be determined and requires extensive further work.

4.3. Comparison with previous studies

APD shortening, probably due to reduced $I_{Ca,L}$, is the most accepted mechanism of contractile dysfunction during early AF [8,12] with a limited role of myolysis [12]. In AF patients, upregulation of the Na^+/Ca^{2+} exchanger [9] and impaired myofibrillar energetics have been identified as candidate mechanisms contributing to atrial contractile dysfunction [10]. SR Ca^{2+} load appears unaltered in atrial myocytes from AF patients [33], probably as a result of PLB hyperphosphorylation and subsequent increase in Serca2a function [34] that likely compensate for the increased SR Ca^{2+} leak via potentially leaky (hyperphosphorylated) RYR2 [35]. However, while in patients hyperphosphorylated PLB results from an increased inhibition of SR-bound PP1 by its endogeneous inhibitor-1, in atrial myocardium of AVB and AF goats PLB phosphorylation appears to be reduced primarily by lower local PKA and CaMKII activity. The distinct alterations and the different underlying mechanism of PLB phosphorylation in AF patients may reflect the influences of concomitant clinical conditions, medication or arrhythmia duration. Our present findings emphasize the need to dissect the specific mechanisms underlying atrial remodeling in different subsets and phenotypes of AF patients.

Dogs undergoing rapid atrial pacing also have preserved SR Ca^{2+} load [11] at low stimulation frequencies. In the present study, SR Ca^{2+} load was unaltered in AVB and AF goats at low frequencies (1 Hz) but significantly reduced at physiological rates (2.5 Hz), emphasizing the need to assess SR Ca^{2+} load–frequency relationships. Recently, increased Ca^{2+} transient amplitude in the presence of decreased atrial contractility has been demonstrated in dilated atria of dogs with heart failure [36]. These findings are in line with reduced myofibril force generation as suggested by our observation of reduced MyBP-C phosphorylation.

4.4. Limitations and implications

We were unable to evaluate cellular ion channel physiology and Ca^{2+} handling in atrial myocytes because isolation of viable myocytes from goat atria required high concentrations of proteases resulting in membrane destabilization and depolarization.

In patients with AF, maximal force generation and Ca^{2+} responsiveness of skinned fibers are unaltered [37,38]. Similar results have been reported in patients with slight atrial dilatation (~+10% in RA major axis) [38]. Thus, reduced MyBP-C and Tn-I phosphorylation in AVB goats may be a transient event in the development of contractile dysfunction, but the exact role of impaired myofilament phosphorylation warrants further investigation. Since AF itself causes moderate atrial enlargement, some aspects of AF-induced atrial contractile dysfunction might result from mechanical factors related to dilatation per se that are difficult to dissect from other arrhythmia-specific mechanisms. Subsequent work with AF induced in the dilated atria of AVB goats could address these aspects more specifically.

Funding

Dutch Heart Foundation (2002.B040, 2005.B112); German Federal Ministry of Education and Research through the Atrial Fibrillation Competence Network (01Gi0204), Canadian Institutes of Health Research; German Research Foundation (BO 1263/9-1); the European Union (NORMACOR Network), a grant from Fondation Leducq (07 CVD 03). HRN was supported by the Deutsche Forschungsgemeinschaft (KFO 196, NE 1460/1-1).

Conflict of interest
None declared.

Acknowledgments

The authors thank Arne van Hunnik, Marion Kuipers, Sarah Hulsmans, Manja Schöne, Annett Opitz, and Sabine Kirsch for excellent technical support and Medtronic Inc. (Bakken Research Center, Maastricht) for providing pacemakers and leads.

Appendix A. Supplementary data

Supplementary data associated with this article can be found, in the online version, at doi:10.1016/j.yjmcc.2008.11.012.

References

[1] Gorelick PB. Stroke prevention. An opportunity for efficient utilization of health care resources during the coming decade. Stroke 1994;25:220–4.
[2] Petty GW, Brown Jr RD, Whisnant JP, Sicks JD, OÆFallon WM, Wiebers DO. Ischemic stroke subtypes: a population-based study of incidence and risk factors. Stroke 1999;30:2513–6.
[3] Di Tullio MR, Sacco RL, Sciacca RR, Homma S. Left atrial size and the risk of ischemic stroke in an ethnically mixed population. Stroke 1999;30:2019–24.
[4] Cabin HS, Clubb KS, Hall C, Perlmutter RA, Feinstein AR. Risk for systemic embolization of atrial fibrillation without mitral stenosis. Am J Cardiol 1990;65:1112–6.
[5] Benjamin EJ, D'Agostino RB, Belanger AJ, Wolf PA, Levy D. Left atrial size and the risk of stroke and death. The Framingham Heart Study. Circulation 1995;92:835–41.
[6] Shi Y, Ducharme A, Li D, Gaspo R, Nattel S, Tardif JC. Remodeling of atrial dimensions and emptying function in canine models of atrial fibrillation. Cardiovasc Res 2001;52:217–25.
[7] Sparks PB, Mond HG, Vohra JK, Yapanis AG, Grigg LE, Kalman JM. Mechanical remodeling of the left atrium after loss of atrioventricular synchrony — a long-term study in humans. Circulation 1999;100:1714–21.
[8] Schotten U, Duytschaever M, Ausma J, Eijsbouts S, Neuberger HR, Allessie M. Electrical and contractile remodeling during the first days of atrial fibrillation go hand in hand. Circulation 2003;107:1433–9.
[9] Schotten U, Greiser M, Benke D, Buerkel K, Ehrenteidt B, Stellbrink C, et al. Atrial fibrillation-induced atrial contractile dysfunction: a tachycardiomyopathy of a different sort. Cardiovasc Res 2002;53:192–201.
[10] Mihm MJ, Yu F, Carnes CA, Reiser PJ, McCarthy PM, Van Wagoner DR, et al. Impaired myofibrillar energetics and oxidative injury during human atrial fibrillation. Circulation 2001;104:174–80.
[11] Kneller J, Sun H, Leblanc N, Nattel S. Remodeling of Ca^{2+}-handling by atrial tachycardia: evidence for a role in loss of rate-adaptation. Cardiovasc Res 2002;54:416–26.
[12] Schotten U, Ausma J, Stellbrink C, Sabatschus I, Vogel M, Frechen D, et al. Cellular mechanisms of depressed atrial contractility in patients with chronic atrial fibrillation. Circulation 2001;103:691–8.
[13] Deroubaix E, Folliguet T, Rücker-Martin C, Dinanian S, Boixel C, Validire P, et al. Moderate and chronic hemodynamic overload of sheep atria induces reversible cellular electrophysiologic abnormalities and atrial vulnerability. J Am Coll Cardiol 2004;44:1918–26.
[14] Neuberger HR, Schotten U, Verheule S, Eijsbouts S, Blaauw Y, van Hunnik A, et al. Development of a substrate of atrial fibrillation during chronic atrioventricular block in the goat. Circulation 2005;111:30–7.
[15] Verheule S, Wilson E, Banthia S, Everett IV TH, Shanbhag S, Sih HJ, et al. Direction-dependent conduction abnormalities in a canine model of atrial fibrillation due to chronic atrial dilatation. Am J Physiol Heart Circ Physiol 2004;287:H634–644.
[16] de Haan S, Greiser M, Harks E, Blaauw Y, van Hunnik A, Verheule S, et al. AVE0118, blocker of the transient outward current (I(to)) and ultrarapid delayed rectifier current (I(Kur)), fully restores atrial contractility after cardioversion of atrial fibrillation in the goat. Circulation 2006;114:1234–42.
[17] Ausma J, Wijffels M, Thoné F, Wouters L, Allessie M, Borgers M. Structural changes of atrial myocardium due to sustained atrial fibrillation in the goat. Circulation 1997;96:3157–63.
[18] Hryshko LV, Stiffel V, Bers DM. Rapid cooling contractures as an index of sarcoplasmic reticulum calcium content in rabbit ventricular myocytes. Am J Physiol 1989;257:H1369–1377.
[19] Popov N, Schmitt M, Schulzeck S, Matthies H. Reliable micromethod for determination of the protein content in tissue homogenates. Acta Biol Med Ger 1975;34:1441–6.
[20] El Armouche A, Boknik P, Eschenhagen T, Carrier L, Knaut M, Ravens U, et al. Molecular determinants of altered Ca^{2+} handling in human chronic atrial fibrillation. Circulation 2006;114:670–80.
[21] Boknik P, Fockenbrock M, Herzig S, Knapp J, Linck B, Luss H, et al. Protein phosphatase activity is increased in a rat model of long-term beta-adrenergic stimulation. Naunyn- Schmiedeberg's Arch Pharmacol 2000;362:222–31.
[22] Christ T, Boknik P, Wohrl S, Wettwer E, Graf EM, Bosch RF, et al. L-type Ca^{2+} current downregulation in chronic human atrial fibrillation is associated with increased activity of protein phosphatases. Circulation 2004;110:2651–7.
[23] Yue L, Feng J, Gaspo R, Li GR, Wang Z, Nattel S. Ionic remodeling underlying action potential changes in a canine model of atrial fibrillation. Circ Res 1997;81:512–25.
[24] Bosch RF, Zeng X, Grammer JB, Popovic K, Mewis C, Kühlkamp V. Ionic mechanisms of electrical remodeling in human atrial fibrillation. Cardiovasc Res 1999;44:121–31.
[25] Li D, Melnyk P, Feng J, Wang Z, Petrecca K, Shrier A, et al. Effects of experimental heart failure on atrial cellular and ionic electrophysiology. Circulation 2000;101:2631–8.
[26] Röcken C, Peters B, Juenemann G, Saeger W, Klein HU, Huth C, et al. Attrial amyloidosis: an arrhythmogenic substrate for persistent atrial fibrillation. Circulation 2002;106:2091–7.
[27] Ausma J, Litjens N, Lenders MH, Duimel H, Mast F, Wouters L, et al. Time course of atrial fibrillation-induced cellular structural remodeling in Atria of the goat. J Mol Cell Cardiol 2001;33:2083–94.
[28] Bers DM. Excitation-Contraction Coupling and Cardiac Contractile Force 2nd edition Dordrecht. the Netherlands: Kluwer; 2001.
[29] Bers DM. Altered cardiac myocyte Ca regulation in heart failure. Physiology (Bethesda) 2006;21:380–7.
[30] Stelzer JE, Patel JR, Moss RL. Protein kinase A-mediated acceleration of the stretch activation response in murine skinned myocardium is eliminated by ablation of cMyBP-C. Circ Res 2006;99:884–90.
[31] El-Armouche A, Pohlmann L, Schlossarek S, Starbatty J, Yeh YH, Nattel S, et al. Decreased phosphorylation levels of cardiac myosin-binding protein-C in human and experimental heart failure. J Mol Cell Cardiol 2007;43:223–9.
[32] Marx SO, Reiken S, Hisamatsu Y, Jayaraman T, Burkhoff D, Rosemblit N, et al. PKA phosphorylation dissociates FKBP12.6 from the calcium release channel (ryanodine receptor): defective regulation in failing hearts. Cell 2000;101:365–76.
[33] Hove-Madsen L, Llach A, Bayes-Genis A, Roura S, Rodriguez FE, Aris A, et al. Atrial fibrillation is associated with increased spontaneous calcium release from the sarcoplasmic reticulum in human atrial myocytes. Circulation 2004;110:1358–63.
[34] Maclennan DH, Kranias EG. Phospholamban: a crucial regulator of cardiac contractility. Nat Rev Mol Cell Biol 2003;4:566–77.
[35] Vest JA, Wehrens XH, Reiken SR, Lehnart SE, Dobrev D, Chandra P, et al. Defective cardiac ryanodine receptor regulation during atrial fibrillation. Circulation 2005;111:2025–32.
[36] Yeh YH, Wakili R, Qi XY, Chartier D, Boknik P, Kääb S, et al. Calcium handling abnormalities underlying atrial arrhythmogenesis and contractile dysfunction in dogs with congestive heart failure. Circ Arrhythmia Electrophysiol 2008;1:93–102.
[37] Narolska NA, Eiras S, van Loon RB, Boontje NM, Zaremba R, Spiegelen B, et al. Myosin heavy chain composition and the economy of contraction in healthy and diseased human myocardium. J Muscle Res Cell Motil 2005;26:39–48.
[38] Eiras S, Narolska NA, van Loon RB, Boontje NM, Zaremba R, Jimenez CR, et al. Alterations in contractile protein composition and function in human atrial dilatation and atrial fibrillation. J Mol Cell Cardiol 2006;41:467–77.